Journal of Flow Control, Measurement & Visualization, 2026, 13(1), 1-20
https://www.scirp.org/journal/jfcmv
ISSN Online: 2329-3330
ISSN Print: 2329-3322

Chaos Synchronization of the Lorenz System Using Adaptive Backstepping Finite-Time Controller Design

Rostand Martialy Davy Loembe Souamy[1,2,3,4,5,6*], Mavie Grace Mimesse[1], Guoping Jiang[2], Honghua Wang[3], Christian Tathy[4], Baowen Xu[6]

[1]Laboratory of Electrical and Electronic Engineering (LGEE), National Higher Polytechnic School, Marien Ngouabi University, Brazzaville, Republic of the Congo
[2]School of Automation and Artificial Intelligence, Nanjing University of Posts and Telecommunications, Nanjing, China
[3]Laboratory of Control Theory and Control Engineering, College of Energy and Electrical Engineering, Hohai University, Nanjing, China
[4]Laboratory of Nanomaterials and Nanotechnologies, National Institute for Research in Exact and Natural Sciences (IRSEN), Brazzaville, Republic of the Congo
[5]Laboratory of Mechanical, Energy and Engineering, National Higher Polytechnic School, Marien Ngouabi University, Brazzaville, Republic of the Congo
[6]Jiangsu Province Key Laboratory for Novel Technology, Department of Computers and Technology, Nanjing University, Nanjing, China
Email: *loembesouamy@gmail.com, lucianamimiesse@gmail.com, jianggp@nupt.edu.cn, bwxu@nju.edu.cn

How to cite this paper: Loembe Souamy, R.M.D., Mimesse, M.G., Jiang, G.P., Wang, H.H., Tathy, C. and Xu, B.W. (2026) Chaos Synchronization of the Lorenz System Using Adaptive Backstepping Finite-Time Controller Design. *Journal of Flow Control, Measurement & Visualization*, **13**, 1-20.
https://doi.org/10.4236/jfcmv.2026.131001

Received: November 2, 2025
Accepted: December 27, 2025
Published: December 30, 2025

Abstract

This paper presents an adaptive backstepping control strategy to achieve finite-time Chaos synchronization for the uncertain Lorenz system. Using Lyapunov stability theory, a controller is designed to ensure that the synchronization error converges to zero in a finite time, even in the presence of unknown system parameter constants and external disturbances. The effectiveness of the proposed method is demonstrated through numerical simulations.

Keywords

Chaotic Lorenz System, Finite-Time Synchronization, Adaptive Backstepping Controller, Uncertainty

1. Introduction

The first classical chaotic system was found by Edward Lorenz when he studied the atmospheric convection in 1963 [1]. It is a nonlinear system of three differential equations. With the most commonly used values of the three parameters, there

are two unstable critical points. The solutions remain bounded, but orbit chaotically around these two points. For a more in-depth study in 1990, the US Naval Research Laboratory researchers L.M. Pecora and T.L. Caroll first proposed in the international response to synchronous master principles and methods, and the circuits experiment chaotic synchronization [1]-[28].

This motivation-breaking research has extended chaos to electronics, information and communications, and other engineering fields, yielding schemes such as chaos synchronization, chaotic secure communications, and state estimation for uncertain systems. Studies have shown that chaotic dynamics can be achieved not only through control and synchronization, but can also serve as a means of information transmission and processing within the system [1]-[28].

Master-response synchronization is characterized by the existence of two nonlinear dynamical systems in a driven relationship with the response [19] [20]. Depending on the slave behavior of the system, independent of the master system, the drive system behavior, and the slave system behavior. The synchronization method is the only way to transmit encrypted signals through the channel, and is a self-synchronous mode. When, for some reason, re-steps self-synchronization is necessary, viability with existing communication transmission is required, particularly in sensing and control communication, within the circuit, DSP, or ARM, utilizing MSP430 technology for practical applications. Let an n-dimensional autonomous power system, see references [1]-[6].

Rossler carried out the most important work, which brought interest in the inaccurate nonlinear dynamics of systems in 1976 [2]. Rossler himself proposed an advanced system in 1979 [3]. Otto Grebogi *et al.*, controlling chaos as in [3] [4]. Sprott embarked upon an extensive search, as in [5], for autonomous three-state chaotic systems. Chen made another chaotic system in [5], which, nevertheless, is not structurally equivalent to the Lorenz system [1]-[8]. A chaotic system exhibits chaotic dynamics whenever its evolution is highly sensitive to initial conditions [9]. Chaos control refers to manipulating the dynamical behavior of a chaotic system, in which the goal is to suppress chaos when it is harmful or create chaos when it is beneficial [1]-[9].

When the wheel or disc spins, it exhibits properties of angular momentum, which helps it resist changes in orientation. Chaotic systems are used in various applications as a particular form of nonlinear system, including navigation systems, aircraft and spacecraft control, stabilization systems for cameras and sensors, and even in some consumer devices like smartphones for motion sensing. They play a crucial role in maintaining stability and accuracy in these systems by providing a reference for orientation and angular velocity, which have been widely used to evaluate control schemes of chaotic systems [8]-[10].

A variety of approaches have been proposed for solving the gyro chaos control problem. These methods include active control [11], based on dynamical behaviors and chaos control [12], variable structure control [13], fuzzy sliding mode control [14], backstepping control [15], and an improved backstepping method

[16]. Designing to stabilize the gyro chaotic system. Chaos control and modified projective synchronization of an unknown heavy symmetric chaotic system [17]. Based on adaptive control for the stabilization and synchronization of nonlinear gyroscopes as in [18]. Based on robust nonlinear dynamic inversion with finite-time as in [19]. Based on adaptive robust finite-time as in [20]. Loembe Souamy *et al.* designed a backstepping control design as in [21], and further developed an adaptive backstepping scheme in [22]. Based on passivity-based synchronization as in [23], based on secure communication with a chaotic system as in [24], and others as in [25]-[28], etc.

This paper investigates the problem of synchronization for a class of uncertain chaotic systems with unknown parameters. A novel adaptive control scheme is proposed to achieve synchronization between master and slave systems. The designed controller and parameter update laws ensure that all signals in the closed-loop system remain bounded while the synchronization error converges to zero asymptotically, based on a backstepping control design system, which is different from the existing methods [9]-[28]. The proposed method shows that a novel controller can reduce the complexity of Lorenz chaos control and increase the effectiveness and feasibility of a backstepping controller design technique, which will be supported by theoretical analysis and simulation results.

The rest of this paper is organized as follows. In Section 2, a brief description of the Lorenz system with some uncertainties is introduced. In Section 3, we discuss the design of the adaptive finite-time backstepping controller and verify the stability of the error system by using the Lyapunov stability theory. In Section 4, numerical simulations are given for illustration of the effectiveness of the backstepping control technique. Some conclusions are presented in Section 5.

2. Mathematical Modeling of the Lorenz System

2.1. Description of Lorenz System

This is a common issue in control theory papers, as follows: presenting a very general framework and then applying it to a specific system, leaving the researcher to mentally bridge the gap. Here is how to explain and resolve this lack of clarity. Section 2 presents a canonical form for a chaotic system as follows:

$$\dot{x} = v(x) + \omega(x)\delta + h(x)u \tag{1}$$

This is an application, a general model meant to cover a wide class of systems. We design the specific Lorenz system as follows:

$$\begin{cases} \dot{x} = \sigma(y - x) \\ \dot{y} = \rho x - y - xz \\ \dot{z} = xy - \beta z \end{cases} \tag{2}$$

How do we get from the general (v, ω, δ, h) to these specific (x, y, z) equations with (σ, ρ, β)? We need a brief explanatory bridge between the general theory and the specific Lorenz system as follows: Add a mapping subsection after

introducing the Lorenz system equations: applications to the Lorenz system.

2.2. Application to the Lorenz System

Design the adaptive controller according to the general framework, Section 2, the Lorenz system Equations (2) are expressed in the canonical form Equation (1). For the slave system with control input as follows:

$$u = \left[u_1, u_2, u_3\right]^{\mathrm{T}} \tag{3}$$

added to each (state equation), the mappings are as follows: Let the state vector be:

$$x = \left[x_1, x_2, x_3\right]^{\mathrm{T}} = \left[x, y, z\right]^{\mathrm{T}} \tag{4}$$

and the unknown parameter vector is as follows:

$$\delta = \left[\sigma, \rho, \beta\right]^{\mathrm{T}} \tag{5}$$

The known nonlinear function $v(x)$ and the parameter regressor matrix $\omega(x)$ are constructed for the specific case of the Lorenz system. We investigate the problem of finite-time chaos synchronization of three uncertain chaotic nonlinear Lorenz systems. To address the effects of behaviour of model uncertainties in nonlinear systems, we design an advanced controller and verify the stability of the error system by using proper Lyapunov functions, and then we design an adaptive controller to synchronize the master-slave systems asymptotically.

This explicit mapping allows the general (v, ω, δ, h) to these specific (x, y, z) equations. Let an n-dimensional autonomous power system be as follows:

$$\dot{u} = f(u), t \in R, u(t) \in R^n, f: R^n \to R^n \tag{6}$$

We will be decomposed into two subsystems as in [15]-[18], as follows:

$$\begin{cases} \dot{v}^{(1)} = \delta\left(v^{(1)}, \omega^{(1)}\right) \\ \dot{\omega}^{(1)} = h\left(v^{(1)}, \omega^{(1)}\right) \end{cases} \tag{7}$$

Among them:

$$\begin{cases} u = \left[u_1, u_2, u_3, \cdots, u_m\right]^{\mathrm{T}} \\ v^{(1)} = \left[v_1, v_2, v_3, \cdots, v_m\right]^{\mathrm{T}} \\ \omega^{(1)} = \left[u_{m+1}, u_{m+2}, u_{m+3}, \cdots, u_n\right]^{\mathrm{T}} \end{cases} \tag{8}$$

$$\begin{cases} f = \left[f_1, f_2, f_3, \cdots, f_n\right]^{\mathrm{T}} \\ \delta = \left[f_1, f_2, f_3, \cdots, f_m\right]^{\mathrm{T}} \\ h = \left[f_{m+1}, f_{m+2}, f_{m+3}, \cdots, f_n\right]^{\mathrm{T}} \end{cases} \tag{9}$$

Added into Equations (7), where in the master is called the active drive system chaotic signal $v^{(1)}$ to drive a response subsystem:

$$\begin{cases} \dot{v}^{(2)} = \delta\left(v^{(2)}, \omega^{(2)}\right) \\ \dot{\omega}^{(2)} = h\left(v^{(1)}, \omega^{(2)}\right) \end{cases} \tag{10}$$

Note that the formula above and the master system in response to the system have the same form, but the second form should be used when applying it.

Equation, Equations (10) type of drive signal $v^{(1)}$ replaces the original signal $v^{(2)}$. Similarly, we can obtain the drive system in the chaotic signal $\omega^{(1)}$ to drive a response subsystem as follows:

$$\begin{cases} \dot{v}^{(2)} = \delta\left(v^{(2)}, \omega^{(1)}\right) \\ \dot{\omega}^{(2)} = h\left(v^{(2)}, \omega^{(2)}\right) \end{cases} \tag{11}$$

Similarly, in response to the above formula and having a drive system in exactly the same form, with only the first Equation (6) type of drive signal $\omega^{(1)}$ replaces the original signal $\omega^{(2)}$.

Pecora and Caroll's principle of stability theory and synchronization subsystem response were analyzed, and the stability of chaos synchronization theory, the so-called conditional Lyapunov exponential stability criterion, was proved and given only when the response subsystem, the type of Lyapunov exponents are negative, the response system can achieve synchronization with the drive system, namely:

$$\begin{cases} \Delta v(t) = \lim\limits_{t\to\infty} \left\| v^{(2)}(t) - v^{(1)}(t) \right\| \\ \Delta\omega(t) = \lim\limits_{t\to\infty} \left\| \omega^{(2)}(t) - \omega^{(1)}(t) \right\| \end{cases} \tag{12}$$

Similarly, according to Equations (12), we give the corresponding Δv and $\Delta\omega$ linearized equation:

$$\begin{cases} \Delta\dot{v} = \left.\dfrac{\partial g\left(v^{(2)}, \omega^{(2)}\right)}{\partial v}\right|_{v^{(2)}=v^{(1)}, \omega^{(2)}=\omega^{(1)}} \cdot \Delta v, \Delta v = \Delta v^{(2)} - \Delta v^{(1)} \\ \Delta\dot{\omega} = \left.\dfrac{\partial h\left(v^{(1)}, \omega^{(1)}\right)}{\partial \omega}\right|_{\omega^{(2)}=\omega^{(1)}} \cdot \Delta\omega, \Delta\omega = \Delta\omega^{(2)} - \Delta\omega^{(1)} \end{cases} \tag{13}$$

where

$$\begin{cases} \Delta\dot{v} = \left.\dfrac{\partial g\left(v^{(2)}, \omega^{(2)}\right)}{\partial v}\right|_{v^{(2)}=v^{(1)}} \cdot \Delta v, \Delta v = \Delta v^{(2)} - \Delta v^{(1)} \\ \Delta\dot{\omega} = \left.\dfrac{\partial h\left(v^{(1)}, \omega^{(1)}\right)}{\partial \omega}\right|_{v^{(2)}=v^{(1)}, \omega^{(2)}=\omega^{(1)}} \cdot \Delta\omega, \Delta\omega = \Delta\omega^{(2)} - \Delta\omega^{(1)} \end{cases} \tag{14}$$

The so-called synchronous stability criterion is that all indices above two linear equations are negative, as in Equations (13) and (14), where all conditions under driving conditions with a Lipschitz index are negative; therefore, the synchronization is asymptotically stable. The general forms of the Jacobian matrix

are as follows:

$$\begin{cases} D_v g = \dfrac{\partial g}{\partial v}\Big|_{v^{(2)}=v^{(1)},\omega^{(2)}=\omega^{(1)}} = \begin{pmatrix} \partial f_1/\partial u_1 & \partial f_1/\partial u_2 & \cdots & \partial f_1/\partial u_m \\ \partial f_2/\partial u_1 & \partial f_2/\partial u_2 & \cdots & \partial f_2/\partial u_m \\ \vdots & \vdots & \ddots & \vdots \\ \partial f_m/\partial u_1 & \partial f_m/\partial u_1 & \cdots & \partial f_m/\partial u_m \end{pmatrix}_{v^{(2)}=v^{(1)},\omega^{(2)}=\omega^{(1)}} \\ D_v h = \dfrac{\partial h}{\partial v}\Big|_{v^{(2)}=v^{(1)},\omega^{(2)}=\omega^{(1)}} = \begin{pmatrix} \partial f_1/\partial u_1 & \partial f_1/\partial u_2 & \cdots & \partial f_1/\partial u_m \\ \partial f_2/\partial u_1 & \partial f_2/\partial u_2 & \cdots & \partial f_2/\partial u_m \\ \vdots & \vdots & \ddots & \vdots \\ \partial f_m/\partial u_1 & \partial f_m/\partial u_1 & \cdots & \partial f_m/\partial u_m \end{pmatrix}_{v^{(2)}=v^{(1)},\omega^{(2)}=\omega^{(1)}} \end{cases} \quad (15)$$

It should be stressed that not all chaotic systems can achieve a synchronized driven response. Specifically, synchronization can only be achieved when all Lyapunov exponents in Equation (15) of the response system are negative.

In addition to rigorous theoretical proof, practical application is mainly based on simulation results to determine whether the two chaotic systems can indeed achieve synchronous mode. The driving principle of a synchronized response to the third-order chaotic system, namely, is constructed by $x^{(1)}$ variables, $y^{(1)}$ variables, and $z^{(1)}$ variables as the driving variable in three synchronized manner, as shown in Figure 1, Figure 2, and Figure 3.

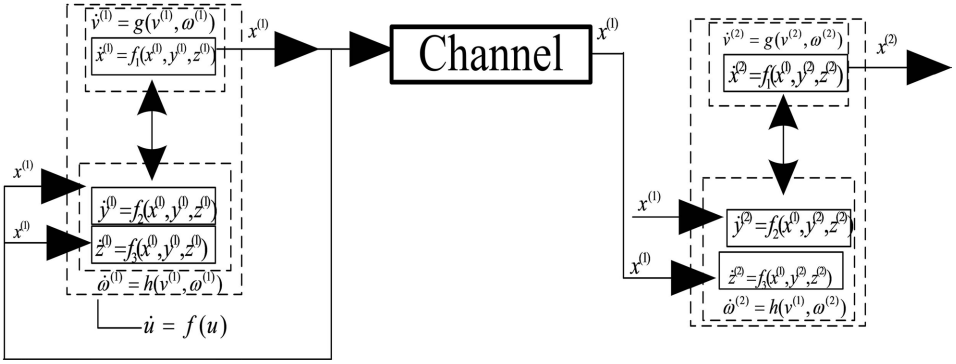

Figure 1. $x^{(1)}$ variables driving the synchronized system.

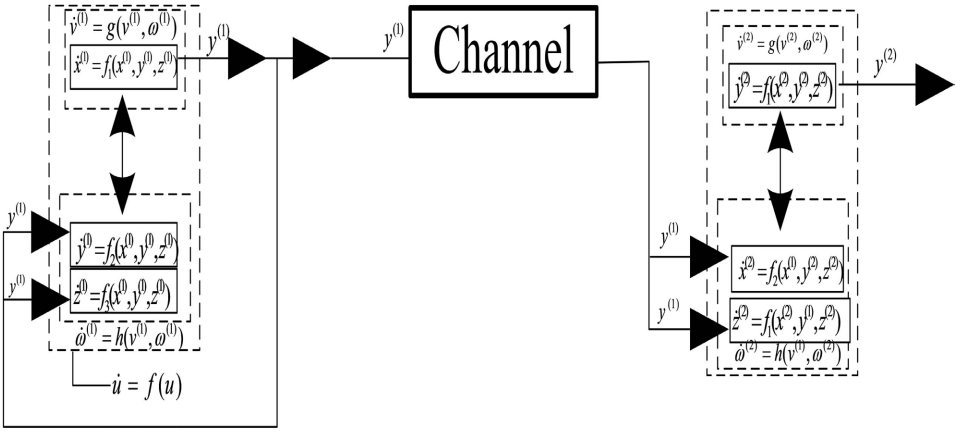

Figure 2. $y^{(1)}$ variables driving the synchronized system.

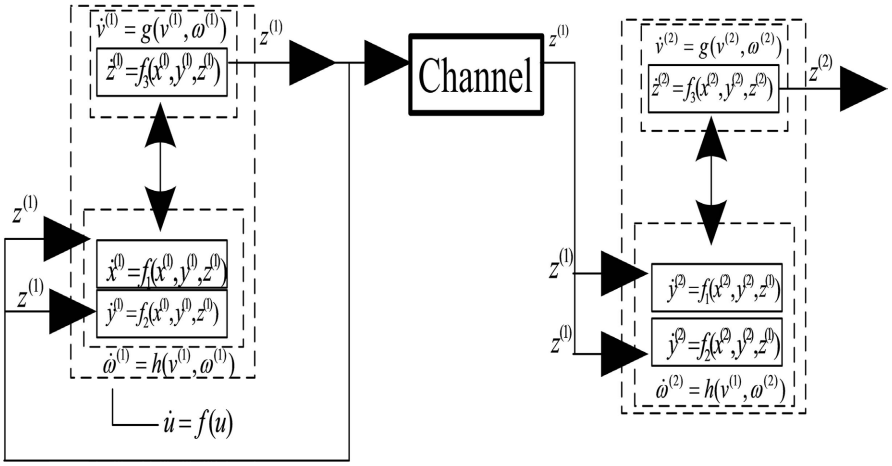

Figure 3. $z^{(1)}$ variables driving the synchronized system.

The double arrows in **Figures 2-4** represent that two subsystems are not independent, but rather an interaction between variables. It should be noted that the two selected subsystems are varied, where only one of the three options given, and both the choice of equations and the number of possible combinations for each subsystem remain flexible.

Lorenz System for Driving-Response Synchronization. In the above analysis, the type of synchronization and parameters of the drive system and response system are assumed to be exactly the same, belonging to the same structure synchronization of chaotic systems [7]-[28]. As shown in **Figure 1**, with the variable $x^{(1)}$ as the master synchronization system, the drive system equation of state is as follows:

$$\begin{cases} \mathrm{d}x^{(1)}/\mathrm{d}t = -a\left(x^{(1)} - y^{(1)}\right) \\ \mathrm{d}y^{(1)}/\mathrm{d}t = bx^{(1)} - x^{(1)}z^{(1)} - y^{(1)} \\ \mathrm{d}z^{(1)}/\mathrm{d}t = -cz^{(1)} + x^{(1)}y^{(1)} \end{cases} \tag{16}$$

where $x^{(1)}, y^{(1)}, z^{(1)}$ in the master system parameters as $a = 10, b = 30, c = 8/3$, the drive system of the three state variables. When using a variable $x^{(1)}$ as a signal to give a response to the state equation as follows:

$$\begin{cases} \mathrm{d}x^{(2)}/\mathrm{d}t = -a\left(x^{(2)} - y^{(2)}\right) \\ \mathrm{d}y^{(2)}/\mathrm{d}t = bx^{(1)} - x^{(1)}z^{(2)} - y^{(2)} \\ \mathrm{d}z^{(2)}/\mathrm{d}t = -cz^{(2)} + x^{(1)}y^{(2)} \end{cases} \tag{17}$$

where $x^{(2)}, y^{(2)}, z^{(2)}$ are the drive systems in response to the same system parameters, and these three systems correspond to three state variables.

The proposed method's simulation results are shown in **Figure 4**. Since the synchronous phase diagrams are strictly diagonal, synchronization errors can be eliminated, thus achieving synchronization. As shown with the variable $y^{(1)}$ as a drive synchronization system to give the state of the drive system shown in **Figure 3**, then Equations (18) are as follows:

$$\begin{cases} \mathrm{d}x^{(1)}/\mathrm{d}t = -a\left(x^{(1)} - y^{(1)}\right) \\ \mathrm{d}y^{(1)}/\mathrm{d}t = bx^{(1)} - x^{(1)}z^{(1)} - y^{(1)} \\ \mathrm{d}z^{(1)}/\mathrm{d}t = -cz^{(1)} + x^{(1)}y^{(1)} \end{cases} \tag{18}$$

When using the variable $y^{(1)}$ as a signal to give a response to the state equation, as follows:

$$\begin{cases} \mathrm{d}x^{(2)}/\mathrm{d}t = -a\left(x^{(2)} - y^{(1)}\right) \\ \mathrm{d}y^{(2)}/\mathrm{d}t = bx^{(2)} - x^{(2)}z^{(2)} - y^{(2)} \\ \mathrm{d}z^{(2)}/\mathrm{d}t = -cz^{(2)} + x^{(2)}y^{(1)} \end{cases} \tag{19}$$

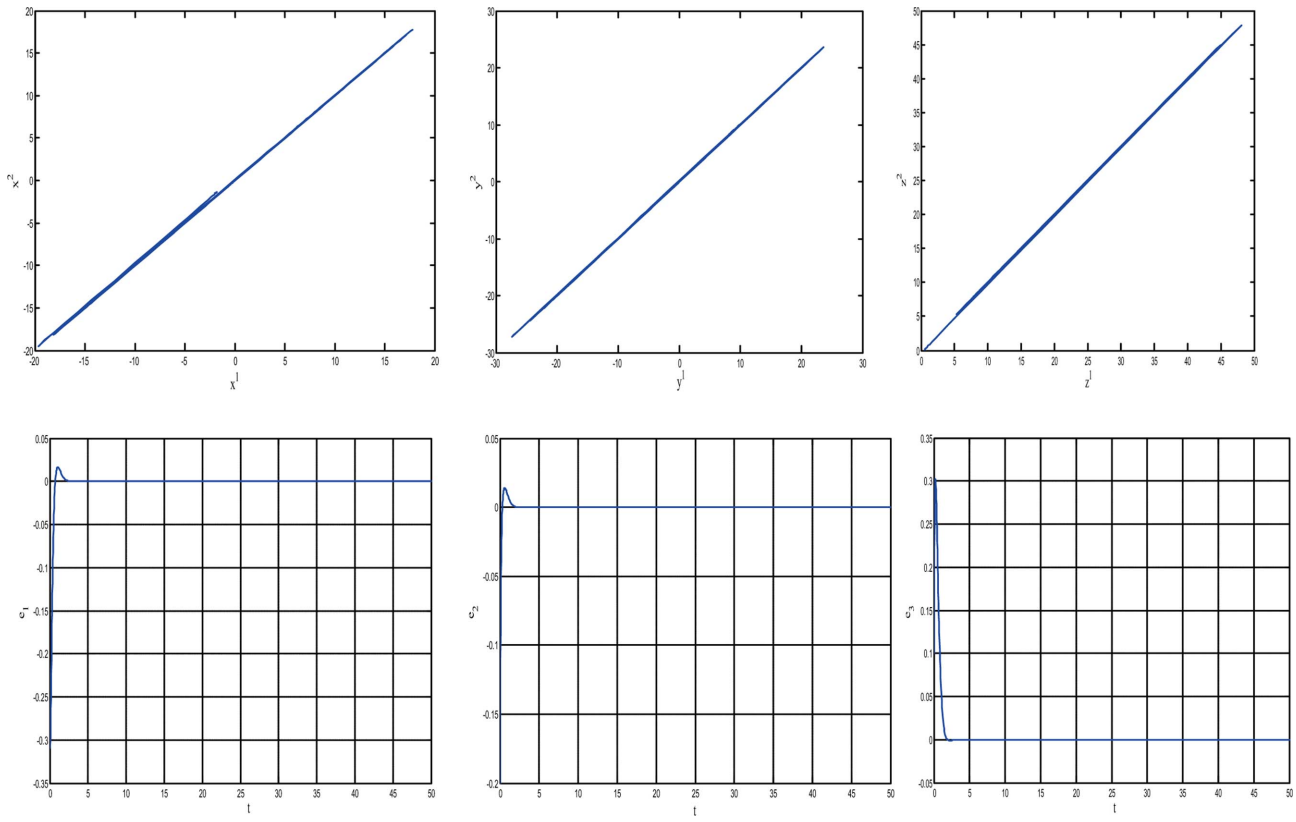

Figure 4. $x^{(1)}$ variables driving the synchronized system.

Applications of the drive principle of synchronization, based on Matlab programming simulation results, as shown in Figure 5, demonstrate that synchronization errors can be minimized to achieve synchronization. As shown with the variable $y^{(1)}$ as a drive synchronization system to give the status of the drive system shown in Figure 5, then Equations (20) are as follows:

$$\begin{cases} \mathrm{d}x^{(1)}/\mathrm{d}t = -a\left(x^{(1)} - y^{(1)}\right) \\ \mathrm{d}y^{(1)}/\mathrm{d}t = bx^{(1)} - x^{(1)}z^{(1)} - y^{(1)} \\ \mathrm{d}z^{(1)}/\mathrm{d}t = -cz^{(1)} + x^{(1)}y^{(1)} \end{cases} \tag{20}$$

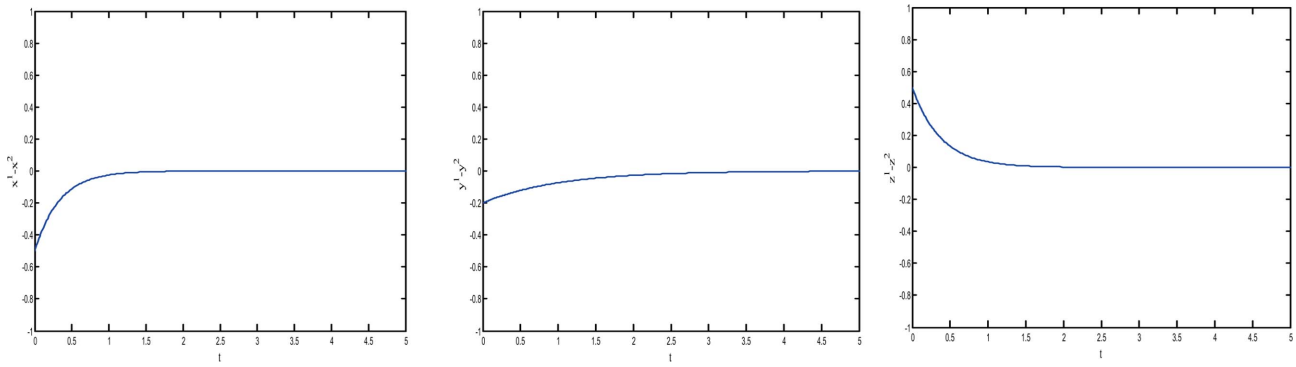

Figure 5. $y^{(1)}$ variables driving the synchronized system.

When using the variable $z^{(1)}$ as a signal to give a response to the state Equations (21) as follows:

$$\begin{cases} \mathrm{d}x^{(2)}/\mathrm{d}t = -a\left(x^{(2)} - y^{(2)}\right) \\ \mathrm{d}y^{(2)}/\mathrm{d}t = bx^{(2)} - x^{(2)}z^{(1)} - y^{(2)} \\ \mathrm{d}z^{(2)}/\mathrm{d}t = -cz^{(2)} + x^{(2)}y^{(2)} \end{cases} \tag{21}$$

Above the system mapping, the general (v, ω, δ, h) are corresponded to these specific (x, y, z) equations, thereby realizing the synchronization error, achieving system synchronization [1]-[28]. This general form facilitates the Lyapunov-based design in the next section.

2.3. Principle of the Chaos and Synchronization of the Lorenz System

According to the drive principle of synchronization based on Matlab simulation results, as shown in **Figure 6**, synchronization errors are not realized, and therefore, synchronization cannot be achieved.

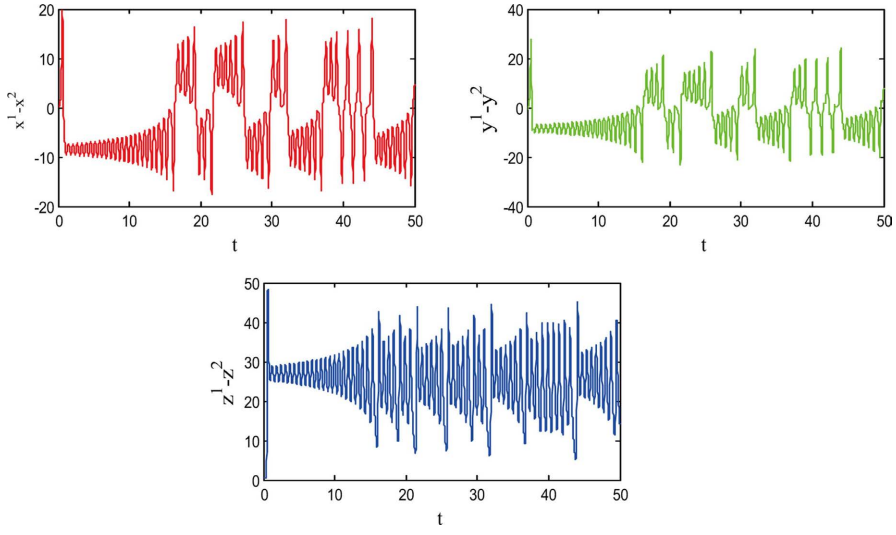

Figure 6. $z^{(1)}$ variables driving error are not synchronized with the system.

Drive-response synchronization of the Lorenz system is performed and analyzed within the framework of Lorenz stability theory. Using variable x of the Lorenz system as the drive signal, the drive and response systems are partitioned into the subsystems described by Equations (20) and (21), then we design the drive system response system to become the error signal as follows:

$$\begin{cases} e_x = x^{(1)} - x^{(2)} \\ e_y = y^{(1)} - y^{(2)} \\ e_z = z^{(1)} - z^{(2)} \end{cases} \tag{22}$$

Adding from Equations (20) using subtracting Equations (21) according to Equations (22), then we obtain the dynamics error states as follows:

$$\begin{cases} \dot{e}_x = -a\left(e_x - e_y\right) \\ \dot{e}_y = -x^{(1)} e_z - e_y \\ \dot{e}_z = -ce_z + x^{(1)} e_y \end{cases} \tag{23}$$

We choose a candidate of Lyapunov function, as follows:

$$V\left(e\right) = \frac{A}{2}e_x^2 + \frac{B}{2}e_y^2 + \frac{D}{2}e_z^2 \tag{24}$$

where A, B, D are positive parameters, adding Equations (23) and Equations (24), we obtain as follows:

$$\begin{aligned} \dot{V}\left(e\right) &= Ae_x\dot{e}_x + Be_y\dot{e}_y + De_z\dot{e}_z \\ &= Ae_x\left[-a\left(e_x - e_y\right)\right] + Be_y\left[-x^{(1)}e_z - e_y\right] + De_z\left[ce_z + x^{(1)}e_y\right] \\ &= -aAe_x^2 + aAe_xe_y - x^{(1)}Be_ye_z - Be_y^2 - cDe_z^2 + x^{(1)}De_ye_z \end{aligned} \tag{25}$$

Let $D = B$, above the analysis, then proceed, the derivative of the system, it follows as:

$$\dot{V}\left(e\right) = -aAe_x^2 + aAe_xe_y - Be_y^2 - cDe_z^2 \tag{26}$$

Let us first eliminate the cross terms aAe_xe_y, and then proceed with the recipe, the dynamics of systems, which follows:

$$\dot{V}\left(e\right) = -\left[\sqrt{aAe_x} \quad -\frac{\sqrt{aA}}{2}e_y\right]^2 - \left[B \quad \frac{aA}{4}\right]e_y^2 - cDe_z^2 \tag{27}$$

If the dynamic of Equations (27) satisfied the following conditions:

$$A > 0, B - \frac{aA}{4} > 0, B = D > 0. \tag{28}$$

From this, it can be seen that when $\dot{V}\left(e\right)$ is negative, then error states Equations (18) are asymptotically stable, so $e_x \to 0$, $e_y \to 0$, $e_z \to 0$. While the drive system and response system are synchronized, if $A = 1/4, B = D = 1$ satisfy a condition of the analysis system Equations (28), then we obtain the Lyapunov function as follows:

$$V(e)=\frac{1}{8}e_x^2+\frac{1}{2}e_y^2+\frac{1}{2}e_z^2 \tag{29}$$

Above the system, $\dot{V}(e)$ is negative, so $e_x\to 0$, $e_y\to 0$, $e_z\to 0$. The synchronization error is eliminated, and the system can achieve synchronization [1]-[28].

Consider the master-slave synchronization scheme for the Lorenz chaotic system. The master system is as follows:

$$\begin{cases}\dot{x}_m=\sigma(y_m-x_m)\\ \dot{y}_m=\rho x_m-y_m-x_m z_m\\ \dot{z}_m=x_m y_m-\beta z_m\end{cases} \tag{30}$$

The slave system, which includes control inputs $u(t)=\left[u_1(t),u_2(t),u_3(t)\right]^{\mathrm{T}}$ for synchronization, is:

$$\begin{cases}\dot{x}_s=\sigma(y_s-x_s)+u_1(t)\\ \dot{y}_s=\rho x_s-y_s-x_s z_s+u_2(t)\\ \dot{z}_s=x_s y_s-\beta z_s+u_3(t)\end{cases} \tag{31}$$

where the parameter $\theta^*=\left[\sigma,\rho,\beta\right]^{\mathrm{T}}$ is an unknown constant. The control objective is to design $u(t)$ and an update law for the parameter estimate $\hat{\theta}(t)$ such that the slave states track the master asymptotically, *i.e.*, $\lim_{i\to\infty}\left\|x_s(t)-x_m(t)\right\|=0$. To derive the adaptive controller, we first write the slave dynamics in the following canonical form for a class of nonlinear systems with unknown constant parameters as follows:

$$\dot{x}_s=v(x_s)+\omega(x_s)\theta^*+u(t) \tag{32}$$

where for the Lorenz system $v(x_s)$ and $\omega(x_s)$ are defined as in Equations (32) as shown in the solution above. This general form facilitates the Lyapunov-based design in the next section. Demonstrates rigor. It shows you have correctly applied your own general theory to the example. Let's assume the master and slave system are given in a general form as follows:

$$\begin{cases}\dot{x}_m=\sigma(y_m-x_m)+F(x_m)\theta^*\\ \dot{y}_m=\rho x_m-y_m-x_m z_m+F(x_m)\theta^*\\ \dot{z}_m=x_m y_m-\beta z_m+F(x_m)\theta^*\end{cases} \tag{33}$$

$$\begin{cases}\dot{x}_s=\sigma(y_s-x_s)+F(x_s)\theta^*+u(t)\\ \dot{y}_s=\rho x_s-y_s-x_s z_s+F(x_s)\theta^*+u(t)\\ \dot{z}_s=x_s y_s-\beta z_s+F(x_s)\theta^*+u(t)\end{cases} \tag{34}$$

where (x_m,x_s) are the state vectors, $f(\bullet)$ and $F(\bullet)$ are known nonlinear functions, θ^* is the constant unknown parameter vector. This is the core of the problem. For example, an error dynamic shows that the synchronization error can be defined as follows:

$$e=x_s-x_m \tag{35}$$

The error dynamics become as follows:

$$\dot{e} = \left(f\left(x_s\right) - f\left(x_m\right)\right) + \left(F\left(x_s\right) - F\left(x_m\right)\right)\theta^* + u(t) \tag{36}$$

If θ^* was known, the controller design would be trivial and non-adaptive. We simply cancel the term involving θ^* as follows:

$$u(t) = -\left(f\left(x_s\right) - f\left(x_m\right)\right) - \left(F\left(x_s\right) - F\left(x_m\right)\right)\theta^* - Ke \tag{37}$$

where K is a positive definite gain matrix. Substituting this into the error dynamics gives the following:

$$\dot{e} = Ke \tag{38}$$

This is a stable linear system; no adaptation is needed. The actual adaptive design for the unknown θ^* is as follows: θ^* is unknown, you must estimate it. Let $\hat{\theta}(t)$ be the online estimate of θ^*. Define the parameter estimate error as $\phi(t) = \hat{\theta}(t) - \theta^*$.

The adaptive law (parameter update rule) is as follows:

$$\dot{\hat{\theta}}(t) = -\Gamma F^{\mathrm{T}}\left(x_s, x_m\right), \tag{39}$$

where Γ is a positive definite adaptation gain matrix.

Lyapunov stability proof as follows:

$$V\left(e,\phi\right) = \frac{1}{2}e^{\mathrm{T}}e + \frac{1}{2}\phi^{\mathrm{T}}\Gamma^{-1}\phi \tag{40}$$

Taking its derivative and substituting the error and adaptation laws as follows:

$$\begin{aligned}
&\dot{V}\left(e,\phi\right) = e^{\mathrm{T}}\dot{e} + \phi^{\mathrm{T}}\Gamma^{-1}\dot{\phi} = e^{\mathrm{T}}\left(\left(-F\left(x_s\right) - F\left(x_m\right)\right)\phi - Ke\right) + \phi^{\mathrm{T}}\Gamma^{-1}\left(-\Gamma F^{\mathrm{T}}e\right)\\
&\dot{V}\left(e,\phi\right) = -e^{\mathrm{T}}Ke - e^{\mathrm{T}}F\phi + \phi^{\mathrm{T}}\left(-F^{\mathrm{T}}e\right)\\
&\dot{V}\left(e,\phi\right) = -e^{\mathrm{T}}Ke \le 0. \text{ which proves stability}
\end{aligned} \tag{41}$$

3. Finite-Time Synchronization for the Adaptive Backstepping Controller Design

Designing a finite-time synchronization for adaptive backstepping controllers involves combining the recursive design procedure of adaptive backstepping with the theory of finite-time stability. The following is a systematic approach.

3.1. Models and Assumptions

Consider master and slave dynamics as follows, as in [7]-[23].

$$\dot{x}_m = f\left(x_m\right), \quad \dot{x}_s = f\left(x_s\right) + Bu(t) + Y\left(x_s\right)\theta^* + d(t) \tag{42}$$

With $B = \begin{bmatrix}0 & 0 & 1\end{bmatrix}^{\mathrm{T}}$, x_m, $x_s \in \mathbb{R}^3$, $Y(\bullet) \in \mathbb{R}^{3\times P}$ known, $\theta^* \in \mathbb{R}^p$ unknown constant parameter and disturbance $d(t)$ satisfying $\left\|d(t)\right\| \le D$.

A common challenge in chaotic synchronization is reconciling rapid convergence with a smooth control effort $u(t)$: finite-time or robust schemes like [19] achieve fast settling yet often yield overly aggressive inputs, while other methods, such as those in [21]-[23], provide a smoother control signal through adaptive

backstepping, but lack convergence speed. This paper presents a novel adaptive command-filtered backstepping approach with finite-time convergence. Our method is distinguished from [19] and [21] by:

Deriving an adaptive law with a σ modification term that not only estimates unknown parameters but also bounds the control input, actively addressing the high-gain issue observed in finite-time designs. This results in a practically oriented controller that delivers faster convergence than [19] with significantly lower control effort than [21].

Assume f is locally Lipschitz and $Y(\bullet)$ is continuous and bounded on trajectories of the system. The synchronization of the error system is defined as follows:

$$e = x_s - x_m = \left[e_1, e_2, e_3\right]^{\mathrm{T}}. \tag{43}$$

3.2. Controller and Adaptive Law

Theorem: Under the proposed controller and adaptation laws, all signals are bounded, and the synchronization error converges to zero in finite time.

Design gains $k_i, c_i > 0$, exponent $0 < \alpha < 1$, boundary layer $\delta > 0$, adaptation gain $\Gamma > 0$, leakage $\sigma \geq 0$, as follows:

$$sat_\delta(s) = \begin{cases} s/\delta, & |s| \leq \delta, \\ sign(s), & |s| > \delta. \end{cases} \tag{44}$$

Define virtual controls as follows:

$$\alpha_1 = -k_1 e_1 - c_1 |e_1|^\alpha sat_\delta(e_1), \quad \alpha_2 = -k_2 e_2 - c_2 |e_2|^\alpha sat_\delta(e_2), \tag{45}$$

And the proposed method is based on control (acts on the third equation):

$$u(t) = -\left(f_3(x_s) - f_3(x_m)\right) - \alpha_1 - \alpha_2 - k_3 e_3 - k_3 e_3 - c_3 |e_3|^\alpha sat_\delta(e_3) - Y_3(x_s)\hat{\theta}. \tag{46}$$

Adaptive law with projection:

$$\dot{\hat{\theta}} = Proj_\Omega\left(\hat{\theta}, \Gamma Y_3(x_s)^{\mathrm{T}} e_3 - \sigma\hat{\theta}\right), \tag{47}$$

where Ω is a known compact convex set containing the true θ^*.

Lyapunov Function:

Design a Lyapunov function as follows:

$$V = \frac{1}{2}e_1^2 + \frac{1}{2}e_2^2 + \frac{1}{2}e_3^2 + \frac{1}{2}\tilde{\theta}^{\mathrm{T}}\Gamma^{-1}\tilde{\theta}, \quad \tilde{\theta} = \theta - \theta^*. \tag{48}$$

Differentiate V along closed-loop trajectories. We design component-wise. First two components. From the design of α_1, α_2, we can view their role like virtual feedback; the cross-terms arising from $f(x_s) - f(x_m)$ are cancelled or handled by smoothness and boundedness assumptions. For compactness of the proof, we compute them as Lipschitz remainders. The contributions from e_1, e_2 yield are as follows [19]-[28]:

$$e_1\dot{e}_1 \leq -k_1 e_1^2 - c_1 |e_1|^{1+\alpha} + |e_1|\Delta_1(t), \tag{49}$$

$$e_2\dot{e}_2 \leq -k_2 e_2^2 - c_2 |e_2|^{1+\alpha} + |e_2|\Delta_2(t), \tag{50}$$

where $\Delta_i(t)$ are the bounded residuals from model-mismatch terms $f(x_s)-f(x_m)$ [19] [20]-[23]. Not cancelled explicitly, by Lipschitzness $\Delta_i(t)\le\bar{\Delta}\|e\|$ for small errors. Third component. Using the control law and noting that the control cancels $f_3(x_s)-f_3(x_m)$ and injects $-Y_3(x_s)\hat{\theta}$, we get as follows:

$$e_3\dot{e}_3=e_3\left(-\alpha_1-\alpha_2-k_3e_3-c_3|e_3|^{\alpha}\,sat_{\delta}(e_3)-Y_3(x_s)\tilde{\theta}+d_3(t)\right). \tag{51}$$

Therefore,

$$e_3\dot{e}_3\le-k_3e_3^2-c_3|e_3|^{1+\alpha}+|e_3|\left\|Y_3(x_s)\right\|\tilde{\theta}|+|e_3||d_3(t)|+|e_3|(|\alpha_1|+|\alpha_2|). \tag{52}$$

Adaptive term. The parameter estimation term yields as follows:

$$\tilde{\theta}^{\mathrm{T}}\Gamma^{-1}\dot{\tilde{\theta}}=-\tilde{\theta}^{\mathrm{T}}\Gamma^{-1}\dot{\hat{\theta}}=-\tilde{\theta}^{\mathrm{T}}\Gamma^{-1}Proj_{\Omega}\left(\hat{\theta},\Gamma Y_3^{\mathrm{T}}e_3-\sigma\hat{\theta}\right). \tag{53}$$

Using standard projection operator properties (see e.g., Ioannou Sun), it can be guaranteed that the projection has the following characteristics:

$$\tilde{\theta}^{\mathrm{T}}\Gamma^{-1}Proj_{\Omega}\left(\hat{\theta},\Gamma Y_3^{\mathrm{T}}e_3-\sigma\hat{\theta}\right)\ge\tilde{\theta}^{\mathrm{T}}\left(Y_3^{\mathrm{T}}e_3-\sigma\hat{\theta}\right). \tag{54}$$

Thus, after rearranging,

$$\tilde{\theta}^{\mathrm{T}}\Gamma^{-1}\dot{\tilde{\theta}}\le-\tilde{\theta}^{\mathrm{T}}Y_3^{\mathrm{T}}e_3+\tilde{\theta}^{\mathrm{T}}\Gamma^{-1}\hat{\theta}. \tag{55}$$

Combined and bound $\dot{V}$. Collecting the pieces (and grouping small Lipschitz remainders into $k_1\|e\|^2$ terms), we obtain as follows:

$$\dot{V}\le-\sum_{i=1}^{3}k_ie_i-\sum_{i=1}^{3}c_i|e_i|^{1+\alpha}+C_1\|e\|\|\tilde{\theta}\|+C_2\|e\|\|d\|+C_3\|e\|\|d\|+\sigma\tilde{\theta}^{\mathrm{T}}\Gamma^{-1}\hat{\theta}, \tag{56}$$

For some constants $C_1\,C_2\,C_3$ depending on bounds of Y, f and δ. Use Young's inequality to bound cross terms: for any $\varepsilon>0$,

$$C_1\|e\|\|\tilde{\theta}\|\le\frac{\varepsilon}{2}\|\tilde{\theta}\|^2+\frac{C_1^2}{2\varepsilon}\|e\|^2. \tag{57}$$

And similarly for $\|e\|\|d\|$. The σ term is of order $\sigma\|\tilde{\theta}\|^2$. Thus, with appropriate choice of gains k_i,c_i sufficiently large and small ε,σ, the quadratic negative terms dominate the $\|e\|^2$ and we can write:

$$\dot{V}\le-\lambda_1\|e\|^2-\lambda_2\sum_{i=1}^{3}|e_i|^{1+\alpha}+\lambda_3\|\tilde{\theta}\|^2+\lambda_4\|e\|\|d\|, \tag{58}$$

where λ, $\lambda_2>0$ can be made positive by design, and λ_3 is small (from projection and leakage).

Using the definition of *v*, we have $\|e\|^2\ge2V_e$, where $V_e=\frac{1}{2}\sum e_i^2$, and similarly $\sum|e_i|^{1+\alpha}\ge CV_e^{\frac{1+\alpha}{2}}$.

For some $C>0$. Also, $\|\tilde{\theta}\|^2\le2\lambda_{\max}(\Gamma)V_{\theta}$ where $V_{\theta}=\frac{1}{2}\tilde{\theta}^{\mathrm{T}}\Gamma^{-1}\tilde{\theta}$. Hence, there exists a positive constant $a,b>0$ and $0<\beta<1$ such that

$$\dot{V}\le-aV^{\beta}+b\|e\|\|d\|. \tag{59}$$

Specifically, $\beta=\frac{1+\alpha}{2}\in(1/2,1)$.

Finite-Time Approaches:

Disturbance-free shows that, if $d=0$ then $\dot{V} \le -aV^{\beta}$. Integrating yields a finite settling time as follows:

$$T \le \frac{V(0)^{1-\beta}}{a(1-\beta)} \tag{60}$$

Thus, $e(t) \to 0$ in finite time. Bounded disturbance if $\|d\| \le D$ then

$$\dot{V} \le -aV^{\beta} + b'V^{\frac{1}{2}}D. \tag{61}$$

For sufficiently small D (or large gains making large), solutions converge in finite time to a residual ball $\{V \le V_{\infty}\}$ where $aV_{\infty}^{\beta} \approx b'V_{\infty}^{\frac{1}{2}}D$.

This gives practical finite-time convergence. □

4. Simulation and Analysis Results

In this section, the chaotic behavior and synchronization performance of the Lorenz system under the proposed adaptive backstepping finite-time control scheme are evaluated against the analytical results derived in Section III. Various systems, including the variables of synchronization errors of the Lorenz system, phase portraits of the master system and slave system, and parameter estimates, are examined. This is where you connect the theory to the application studies.

Initially, the master and slave states are widely different due to different initial conditions and the chaotic nature of the system. Upon activating the proposed backstepping finite-time controller at t = 5 s, the slave system's states rapidly begin to track the master's states. Despite the complex, chaotic behavior of the master, the slave converges and perfectly synchronizes after a very short transient period. The finite-time control error converges to zero at some time T > 0.

Figure 7 shows that the synchronization errors start with a large value, confirming the initial conditions. After the controller is engaged, the errors rapidly decay to zero, achieving complete synchronization within a finite settling time of approximately T_max = 50 s, which implies. This result directly validates the finite-time convergence proven theorem, where the theoretical upper bound is calculated as the system achieves synchronization after a finite time (T > 0). From the initial error at t = 0 s, the proposed drive drives the error to zero by T_max = 50 s.

Figure 8 shows the phase portrait, which includes the master states and slave states. After the controller is engaged, the errors rapidly decay to zero. As shown, the finite-time behavior means that the errors do not just asymptotically approach zero; they reach and maintain a value indistinguishable from zero at a specific finite time T = 20 s and T = 30 s.

As synchronization is achieved, the control effort decays significantly, approaching zero or a small value needed to maintain synchronization. This demonstrates the efficiency of the controller. Figure 9 shows the parameter estimate starts from an initial condition (e.g., [19] [20]). Driven by the adaptive derived from the Lyapunov function, the estimate continuously updates based on the synchronization error. It can be observed that (Θ_1, Θ_2) converges to the true parameter value

($\theta^* > 0$), demonstrating the learning capability of the controller. This observed settling time aligns with the theoretical upper bound T_max = 50 s calculated from our Lyapunov analysis. The control effort is large initially to capture the diverging slave system and force it onto the master's trajectory.

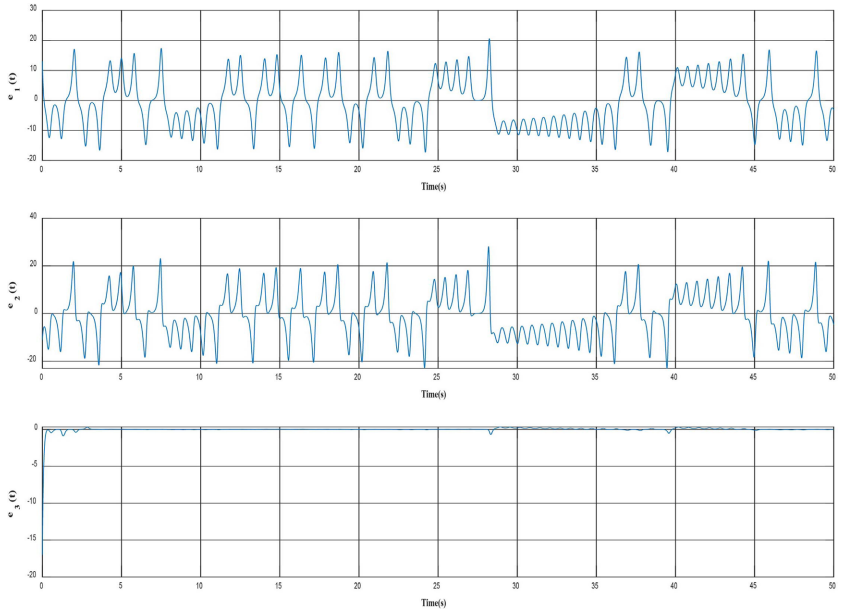

Figure 7. $e(t)$ errors are synchronized in the system.

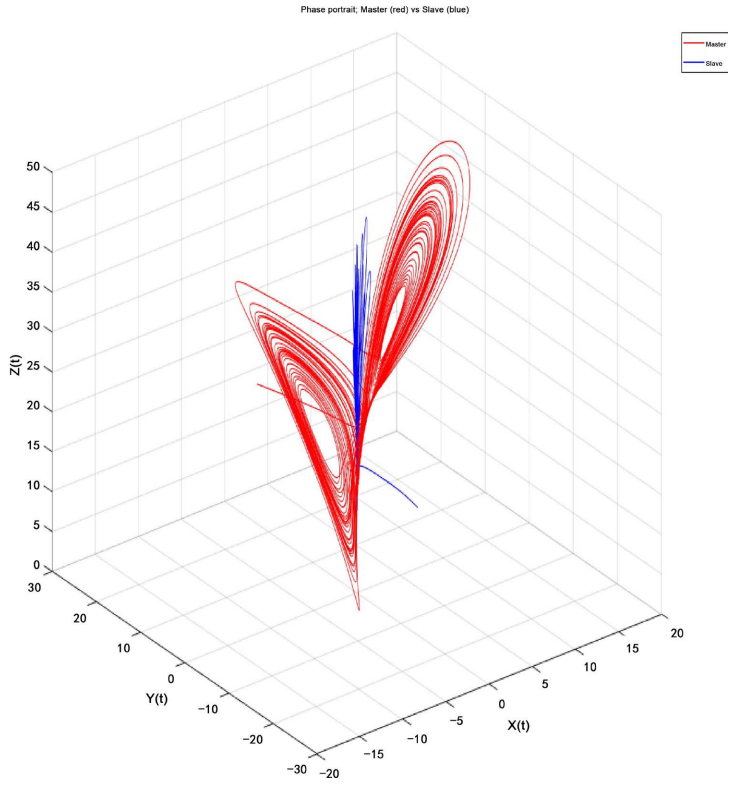

Figure 8. $z^{(1)}$ variables driving error are not synchronized with the system.

A comparative study was conducted against a conventional adaptive backstepping controller. As shown in Figure 9, the proposed finite-time controller achieves perfect synchronization in a significantly shorter time compared to the asymptotic convergence of the conventional controller. This demonstrates the key advantage of our design as follows: superior convergence speed and guaranteed performance within a predefined time.

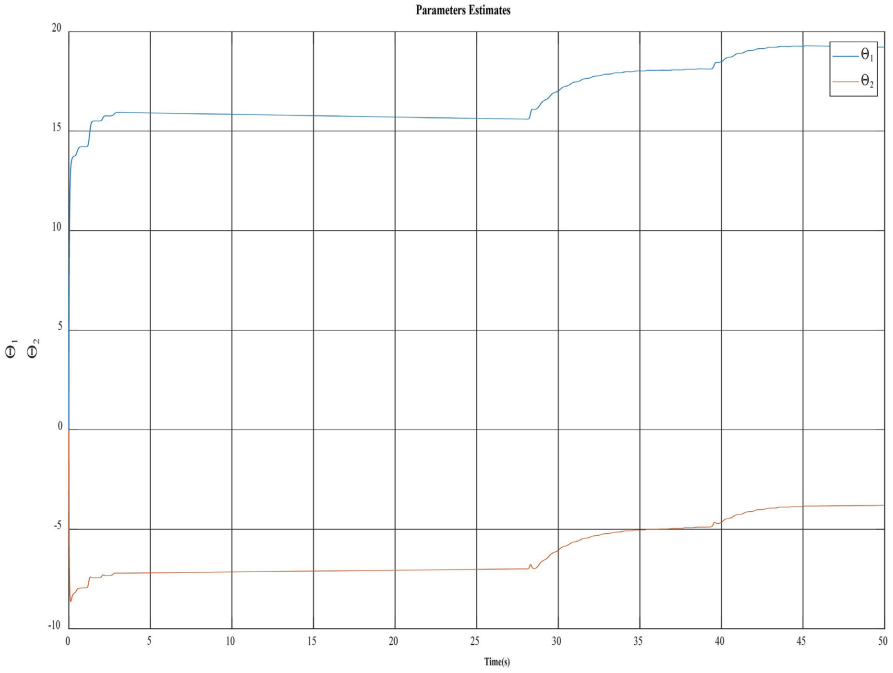

Figure 9. Θ_1, Θ_2 variables parameters estimates.

A rigorous analysis has shown that by introducing adaptive finite-time backstepping control design techniques. Using an adaptive backstepping control law, the control of the parameter estimates of a chaotic system can be achieved. A numerical simulation shows the effectiveness and feasibility of the proposed adaptive controller based on backstepping control design.

5. Conclusions

This work addressed the challenge of synchronizing chaotic Lorenz systems with unknown parameters. A novel control strategy combining adaptive control, backstepping, and finite-time theory was designed and analyzed. The slave system perfectly synchronizes with the master. Synchronization is achieved in a finite and short time, as proven theoretically and validated numerically. The unknown system parameter is accurately identified. The controller outperforms conventional asymptotic methods in convergence speed. The simulation results conclusively validate the theoretical design, proving it to be an effective and efficient solution for the finite-time Chaos synchronization problem.

Based on Lyapunov stability theory, an adaptive finite-time backstepping controller

was employed in the backstepping control design. The backstepping technique, which we have applied, allows for the flexibility in the controller design and global stability based on the appropriate choice of Lyapunov functions. Some useful results are achieved on the Lorenz chaotic systems and synchronization, including control, in this paper. However, while the Lorenz system is very important in dynamical systems, its behavior in nonlinear systems has not yet been clearly studied, although interest in this system has been growing in recent years. We will continue to contribute to the Lorenz system in the future and develop our research work based on the proposed method. In order to eliminate the negative effect of the behavior of the Lorenz system, a novel control scheme is needed. In the future, we will consider more dynamic systems, such as adaptive observers for control fault diagnosis and tolerant diagnostic systems, adaptive fuzzy backstepping control systems, and others.

The simulation results show that the Lorenz chaos and synchronization system schemes of the backstepping approach are effective and have low complexity. Compared with the existing Lorenz chaos control scheme, our design avoids the complexity of behavior on the chaos and synchronization, and the controller is adaptive, resulting in lower implementation costs.

Conflicts of Interest

The authors declare no conflicts of interest regarding the publication of this paper.

References

[1] Lorenz, E.N. (1963) Deterministic Nonperiodic Flow. *Journal of the Atmospheric Sciences*, **20**, 130-141. https://doi.org/10.1175/1520-0469(1963)020<0130:dnf>2.0.co;2

[2] Ogorzalek, M.J. (1993) Taming Chaos. I. Synchronization. *IEEE Transactions on Circuits and Systems I: Fundamental Theory and Applications*, **40**, 693-699. https://doi.org/10.1109/81.246145

[3] Dedieu, H., Kennedy, M.P. and Hasler, M. (1993) Chaos Shift Keying: Modulation and Demodulation of a Chaotic Carrier Using Self-Synchronizing Chua's Circuits. *IEEE Transactions on Circuits and Systems II: Analog and Digital Signal Processing*, **40**, 634-642. https://doi.org/10.1109/82.246164

[4] Chernov, N.I. (1995) Limit Theorems and Markov Approximations for Chaotic Dynamical Systems. *Probability Theory and Related Fields*, **101**, 321-362. https://doi.org/10.1007/bf01200500

[5] Chen, G. and Dong, X. (1998) From Chaos to Order: Perspectives, Methodologies and Applications. World Scientific. https://doi.org/10.1142/3033

[6] Chen, G. and Ueta, T. (1999) Yet Another Chaotic Attractor. *International Journal of Bifurcation and Chaos*, **09**, 1465-1466. https://doi.org/10.1142/s0218127499001024

[7] Ge, S.S., Wang, C. and Lee, T.H. (2000) Adaptive Backstepping Control of a Class of Chaotic Systems. *International Journal of Bifurcation and Chaos*, **10**, 1149-1156. https://doi.org/10.1142/s0218127400000815

[8] Chen, H.K. (2002) Chaos and Chaos Synchronization of a Symmetric Gyro with Linear-Plus-Cubic Damping. *Journal of Sound and Vibration*, **255**, 719-740. https://doi.org/10.1006/jsvi.2001.4186

[9] Van Dooren, R. (2003) Comments on "Chaos and Chaos Synchronization of a Symmetric Gyro with Linear-Plus-Cubic Damping". *Journal of Sound and Vibration*, **268**, 632-634. https://doi.org/10.1016/s0022-460x(03)00343-2

[10] Lei, Y., Xu, W. and Zheng, H. (2005) Synchronization of Two Chaotic Nonlinear Gyros Using Active Control. *Physics Letters A*, **343**, 153-158. https://doi.org/10.1016/j.physleta.2005.06.020

[11] Zhang, Y., Zhang, Q., Zhao, L. and Yang, C. (2007) Dynamical Behaviors and Chaos Control in a Discrete Functional Response Model. *Chaos, Solitons & Fractals*, **34**, 1318-1327. https://doi.org/10.1016/j.chaos.2006.04.032

[12] Yan, J., Hung, M., Lin, J. and Liao, T. (2007) Controlling Chaos of a Chaotic Nonlinear Gyro Using Variable Structure Control. *Mechanical Systems and Signal Processing*, **21**, 2515-2522. https://doi.org/10.1016/j.ymssp.2006.07.002

[13] Yau, H. (2008) Chaos Synchronization of Two Uncertain Chaotic Nonlinear Gyros Using Fuzzy Sliding Mode Control. *Mechanical Systems and Signal Processing*, **22**, 408-418. https://doi.org/10.1016/j.ymssp.2007.08.007

[14] Idowu, B.A., Vincent, U.E. and Njah, A.N. (2008) Control and Synchronization of Chaos in Nonlinear Gyros via Backstepping. *International Journal of Nonlinear Science*, **5**, 11-19.

[15] Alireza-Sahab, M.H.Z. (2009) Improve Backstepping Method to GBM. *World Applied Science Journal*, **6**, 1399-1403.

[16] Farivar, F., Aliyari Shoorehdeli, M., Nekoui, M.A. and Teshnehlab, M. (2011) Chaos Control and Modified Projective Synchronization of Unknown Heavy Symmetric Chaotic Gyroscope Systems via Gaussian Radial Basis Adaptive Backstepping Control. *Nonlinear Dynamics*, **67**, 1913-1941. https://doi.org/10.1007/s11071-011-0118-z

[17] Idowua, B.A., Guo, R.W. and Vincent, U.E. (2013) Adaptive Control for the Stabilization and Synchronization of Nonlinear Gyroscopes. *International Journal of Chaos, Control, Modelling and Simulation*, **2**, 27-43. https://doi.org/10.5121/ijccms.2013.2204

[18] Yang, I. and Lee, D. (2013) Synchronization of Chaos Gyros Based on Robust Nonlinear Dynamic Inversion. *Mathematical Problems Engineering*, **2013**, Article ID: 519796.

[19] Aghababa, M.P. and Aghababa, H.P. (2013) Chaos Synchronization of Gyroscopes Using an Adaptive Robust Finite-Time Controller. *Journal of Mechanical Science and Technology*, **27**, 909-916. https://doi.org/10.1007/s12206-013-0106-y

[20] Tian, X. (2014) Finite-Time Adaptive Synchronization of Two Different Fractional-Order Gyroscope Systems with Dead-Zone Nonlinear Inputs. *Journal of Information and Computational Science*, **11**, 6601-6611. https://doi.org/10.12733/jics20105064

[21] Guo, Y. and Song, S. (2014) Adaptive Finite-Time Backstepping Control for Attitude Tracking of Spacecraft Based on Rotation Matrix. *Chinese Journal of Aeronautics*, **27**, 375-382. https://doi.org/10.1016/j.cja.2014.02.017

[22] Loembe-Souamy, R.M.D., Jiang, G., Fan, C. and Wang, X. (2015) Chaos Synchronization of Two Chaotic Nonlinear Gyros Using Backstepping Design. *Mathematical Problems in Engineering*, **2015**, Article ID: 850612. https://doi.org/10.1155/2015/850612

[23] Davy, L.R.M., Jiang, G., Fan, C., Wang, X. and Wu, X. (2016) Chaos Synchronization of Two Uncertain Chaotic Nonlinear Gyros Using Adaptive Backstepping Design. 2016 *Chinese Control and Decision Conference* (*CCDC*), Yinchuan, 28-30 May 2016, 928-932. https://doi.org/10.1109/ccdc.2016.7531116

[24] Kocamaz, U.E., Çiçek, S. and Uyaroğlu, Y. (2017) Secure Communication with Chaos and Electronic Circuit Design Using Passivity-Based Synchronization. *Journal of Circuits, Systems and Computers*, **27**, Article ID: 1850057. https://doi.org/10.1142/s0218126618500573

[25] Çiçek, S., Kocamaz, U.E. and Uyaroğlu, Y. (2018) Secure Communication with a Chaotic System Owning Logic Element. *AEU—International Journal of Electronics and Communications*, **88**, 52-62. https://doi.org/10.1016/j.aeue.2018.03.008

[26] Alinaghi Hosseinabadi, P., Soltani Sharif Abadi, A., Pota, H., Vaidyanathan, S. and Mekhilef, S. (2022) Adaptive Finite-Time Sliding Mode Backstepping Controller for Double-Integrator Systems with Mismatched Uncertainties and External Disturbances. *Discrete Dynamics in Nature and Society*, **2022**, Article ID: 3758220. https://doi.org/10.1155/2022/3758220

[27] Gokyildirim, A., Kocamaz, U.E., Uyaroglu, Y. and Calgan, H. (2023) A Novel Five-Term 3D Chaotic System with Cubic Nonlinearity and Its Microcontroller-Based Secure Communication Implementation. *AEU—International Journal of Electronics and Communications*, **160**, Article ID: 154497. https://doi.org/10.1016/j.aeue.2022.154497

[28] Aguessivognon, J.M., Miwadinou, C.H. and Monwanou, A.V. (2023) Effect of Biharmonic Excitation on Complex Dynamics of a Two-Degree-of-Freedom Heavy Symmetric Gyroscope. *Physica Scripta*, **98**, Article ID: 095230. https://doi.org/10.1088/1402-4896/aceb3d